Parameterized Modular Inverse Reinforcement Learning

APPROVED BY

SUPERVISING COMMITTEE:

Dana Ballard, Supervisor

Peter Stone

Parameterized Modular Inverse Reinforcement Learning

by

Shun Zhang, B.S.

THESIS

Presented to the Faculty of the Graduate School of

The University of Texas at Austin

in Partial Fulfillment

of the Requirements

for the Degree of

MASTER OF SCIENCE

THE UNIVERSITY OF TEXAS AT AUSTIN

August 2015

Acknowledgments

I wish to thank the multitudes of people who helped me. Time would fail me to tell of ...

Parameterized Modular Inverse Reinforcement Learning

Shun Zhang, M.A.
The University of Texas at Austin, 2015

Supervisor: Dana Ballard

Table of Contents

List of Tables

List of Figures

Chapter 1

Introduction

Chapter 2

Modular Inverse Reinforcement Learning

2.1 Markov Decision Process

In this paper, we represent Markov Decision Process (MDP) as a tuple of five elements, (S, A, P, R, γ), where S is the set of states; A is the set of actions; $P : S \times A \times S \to \mathcal{R}$ denotes the probability of a state-action-state transition; $R : S \to \mathcal{R}$ represents the reward upon reaching a state; γ is the discount factor in the range of $[0, 1]$.

A policy is a mapping $\pi : S \to A$. A value of a state, given a policy, denoted as V^π, is the accumulated discounted rewards by following π.

$$V^\pi(s) = R(s) + \mathrm{E}[\gamma R(s_1), \gamma^2 R(s_2) + \cdots | \pi]$$

, where $s_1, s_2, \cdots$ are the states by following policy π. Or recursively,

$$V^\pi(s) = R(s) + \gamma \sum_{s'} P(s, \pi(s), s') V^\pi(s')$$

, which is known as Bellman Equation [**?**]. The goal is to find the optimal policy π^* so that $V^{\pi^*}(s) \geq V^\pi(s)$ for all s and for all π. We denote V^{π^*} as V^*.

2.2 Modular Reinforcement Learning

2.2.1 Factored Markov Decision Process

One common issue about solving an MDP is the curse of dimensionality. In a large state space, we lack efficient algorithms to find optimal policies. One promising probability to solve this problem is to decompose the state space. We will discuss later in the literature review section on ways proposed to solve this problem. In this section, we consider a factored approach. We represent $S = S_1 \times S_2 \times \cdots \times S_m$, where S_i is the i-th state component. The transition function can be represented as $P(S_i'|S_1, \cdots, S_m, a)$, where S' is the state in the next time step. The correlation between the state components are supposed to be sparse, so S_i' should be independent from the most state components [**?**].

For example, consider a domain in which a robot delivers coffee to a student in his office. The state representation can contain the location of the robot, whether the robot gets a coffee, and whether the robot gets wet.

2.2.2 Modular Reinforcement Learning

A **module class** is a decomposition of the original MDP, denoted by module MDP $\langle S^{(n)}, A, P^{(n)}, R^{(n)}, \gamma^{(n)} \rangle$, where n is the index of this module class. For example, in a navigation task, one module class could be avoiding obstacles. Each module class is a simpler problem so that its value function and policy can be learned or calculated more efficiently. Let N be total number of module classes. One important property of our decomposition is that the

same action space is shared among modules. Hence modular RL algorithms assume global Q values can be obtained by summing up module Q values [31, 33]:

$$Q(s_t, a_t) = \sum_{n=1}^{N} Q^{(n)}(s_t^{(n)}, a_t) \tag{2.1}$$

In an environment, there can be multiple **module instances** of one module class at any given time, e.g., several prizes to be collected, or a few obstacles nearby to avoid. We denote the number of instances of each module class at time t by $M_t^{(1)}, \ldots, M_t^{(N)}$. We generalize the above equation to the case when there are multiple instances of each module class. Suppose the action-value of instance m of module class n at time t is denoted by $Q^{(n)}(s_t^{(n,m)}, a_t)$:

$$Q(s_t, a_t) = \sum_{n=1}^{N} \sum_{m=1}^{M_t^{(n)}} Q^{(n)}(s_t^{(n,m)}, a_t) \tag{2.2}$$

We will use $Q^{(n)}$ to denote module Q values of the nth module and Q without superscription to denote global Q values.

2.3 Modular Inverse Reinforcement Learning

Bayesian inverse reinforcement learning is motivated by the fact that rewards are generally sparse. It aims at recovering all the rewards in the domain. Given a limited number of samples, the observed policy can be optimal for many reward functions. In most real world problems, we are not completely ignorant about what the expert aims at. Instead, we propose some hypothesis on what the expert could be doing, and find out which subset of hypothesis

is consistent with the expert's behavior. This motivates employing *modular MDPs* that we define below.

We assume that the Q function is the sum of the Q functions of the modular MDPs, that is, $Q(s,a) = \sum_i Q_i(s,a)$, where the Q_i is the i-th module. Usually we assume the state representation is factored so that a module only depends on a subset of state components.

We follow the probabilistic formulation of IRL developed by [26] and revise the modular IRL algorithm in [30]. This approach assumes that the higher the Q-value for an action a_t in state s_t, the more likely state-action pair (s_t, a_t) is observed. Let η denote the confidence level in optimality (the extent to which an agent follows the optimal policy). In this section, we propose an approach to define modular MDPs in a flexible way. This work follows closely the work by [30], extending it to handle multiple instances of each module, learning the discount factors, and deriving a different objective function.

An MDP, M, can be denoted as a set of sub-MDPs, or modules, with a configuration parameter vector for each module. Concretely, $M = \{M_i(p_i)\}$. The i-th module is denoted as $M_i(p_i)$, where p_i is a vector that configures the i-th module. The configuration parameter makes the modules flexible, but does not affect the foundamental behaviors of the modules. For example, consider a domain with targets, and an agent can move in the domain to collect targets. Let M_1 be the module of target collection. Then its configuration parameter can be the reward of the target, and the discount factor ($p_1 = (r_1, \gamma_1)$). Note

that r_1 can be either positive or negative. So this module can capture both the behaviors of target collection and target avoidance.

$$\max_p \prod_t \frac{e^{\eta Q(s^{(t)},a^{(t)})}}{\sum_b e^{\eta Q(s^{(t)},b)}} \tag{2.3}$$

, which is equivalent to

$$\max_p \log \prod_t \frac{e^{\eta Q(s^{(t)},a^{(t)})}}{\sum_b e^{\eta Q(s^{(t)},b)}} \tag{2.4}$$

$$= \max_p \sum_t (\eta Q(s^{(t)}, a^{(t)}) - \log \sum_b e^{\eta Q(s^{(t)},b)}) \tag{2.5}$$

$$= \max_p \sum_t (\eta \sum_i Q_i(s^{(t)}, a^{(t)}) - \log \sum_b e^{\eta \sum_i Q_i(s^{(t)},b)}) \tag{2.6}$$

Chapter 3

Literature Review

3.1 Overview

3.2 Forward Model

Abstraction on MDP

- Aggregate states: feature extraction.
- Aggregate actions: **option**.
- Decompose transition: factored MDP.
- Decompose value (abstract MDP): **HAM, hierarchical RL, modular RL**.

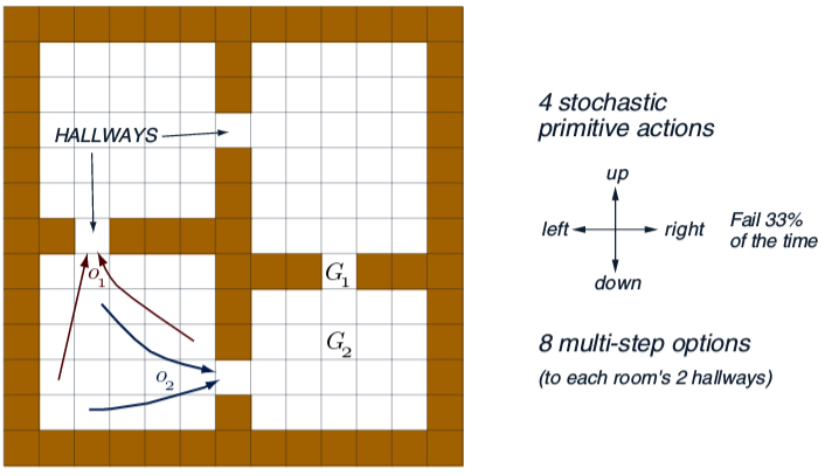

MDP with Option

Approaches	State	Action	Transition	Reward
MDP with Option		Aggregated actions		
Factored MDP	Decomposed		Decomposed	Decomposed or not
HAM	sub-MDP			
Hierarchical RL		Recursive options		Value of options
Modular RL	Decomposed			Decomposed

Table 3.1: Overview of decomposition or aggregation of the components of MDP.

- Option: (start state, policy, termination condition).
- State: S.
- Action: A, O.
- Transition: $P : S \times \{A, O\} \times S \to \mathcal{R}$.
- Reward: $R : S \times \{A, O\} \times S \to \mathcal{R}$.

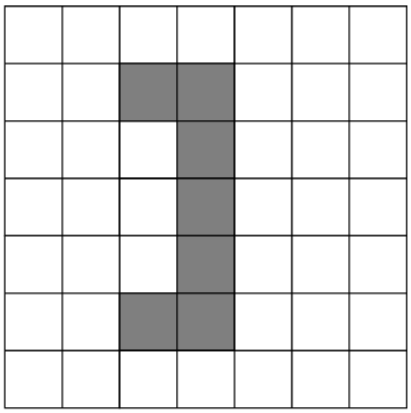

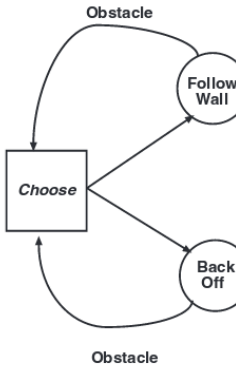

Hierarchies of Abstract Machines (HAM)

- State machine of MDPs.

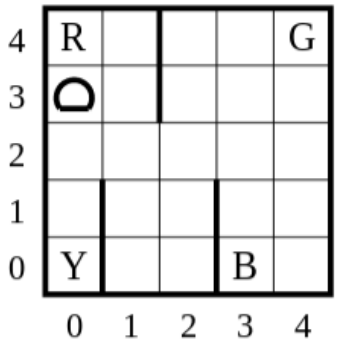

Hierarchical RL

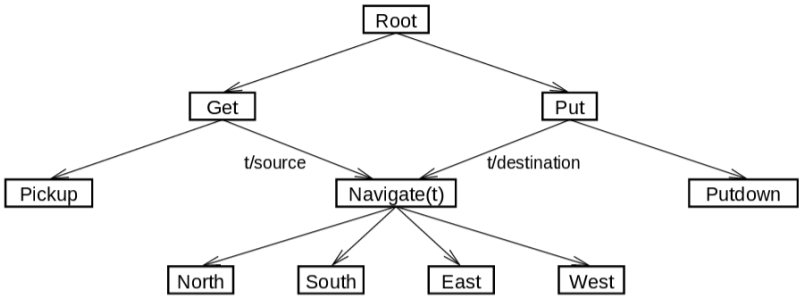

Hierarchical RL MDP:

- State: $\mathcal{S}$.
- Action: $\mathcal{A}$.
- Transition: $\mathcal{T}$.
- Reward: $\mathcal{R}$.

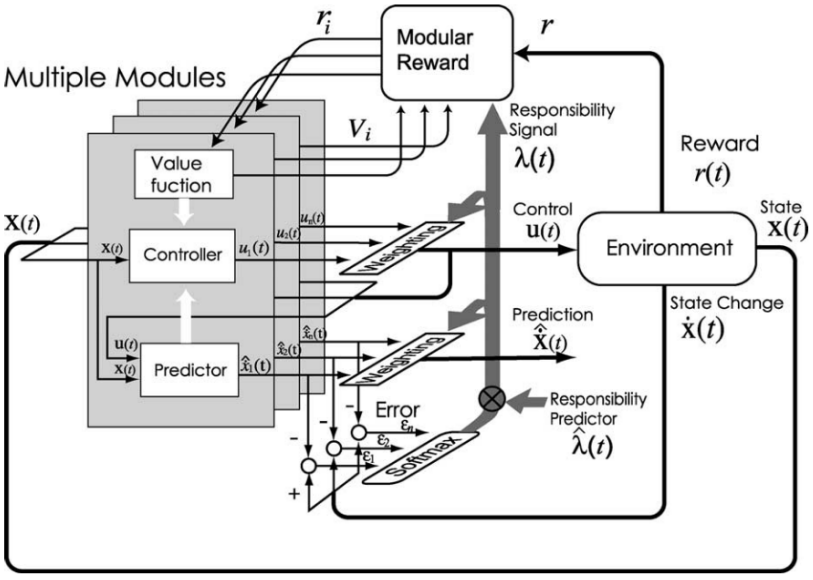

Fig. 1. MMRL.

Modular RL

MDP:

- State: $S_1 \times S_2 \cdots \times S_M$.
- Action: A.
- Transition: $P_1 \times P_2 \cdots \times P_M$.
- Reward: $R_1 \times R_2 \cdots \times R_M$.

3.3 Advances in Recent Work

Not fix a model.

Learn the components,

Dynamic.

Chapter 4

Evaluations and Applications

4.1 Preliminary Evaluation

4.1.1 Modular versus Non-modular Inverse Reinforcement Learning

We compare our algorithm with non-modular Bayesian inverse reinforcement learning [26] to demonstrate the sample efficiency advantage of the modular approach. We use a Laplacian prior in Bayesian IRL since the rewards are sparse. In Figure 4.1, we report the sample efficiency of modular IRL versus Bayesian IRL. There are 4 modular classes and each has 4 instances. We run both algorithms with different number of samples (state-policy pairs). We then compare the policies generated using the learned rewards. Policy agreement is defined as the proportion of the states that have the same policy as the ground truth. We use the metric of policy agreement in our comparison since the outputs of these two algorithms are weights and rewards, which can not be directly compared. Our observation is that modular IRL obtained nearly 100% policy agreement with far fewer samples compared to the non-modular approach.

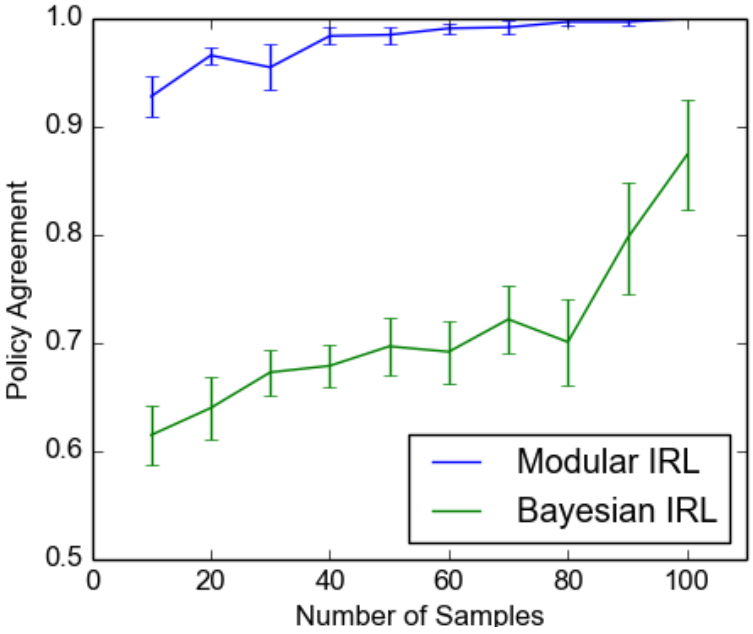

Figure 4.1: Modular IRL vs Bayesian IRL on sample efficiency, measured by policy agreement.

4.2 Human Experiment Results

In this section, we report results from the human virtual navigation experiment. We hypothesize that behavior data can be modeled by our maximum likelihood modular IRL framework and test against baseline models. Figure 4.2 shows the experimental setup. The human subjects wore a binocular head-mounted display. The subjects' eye, head, and body motion were tracked while walking through a virtual room. The subjects were asked to collect the targets (blue spheres) by intercepting them, follow the path (the gray line), and avoid the obstacles (red cubes). Thus this domain has three module classes: following the path, collecting targets, and avoiding obstacles.

This general paradigm has been used to evaluate modular IRL algorithms [30] and to study human navigation and gaze behavior [40].

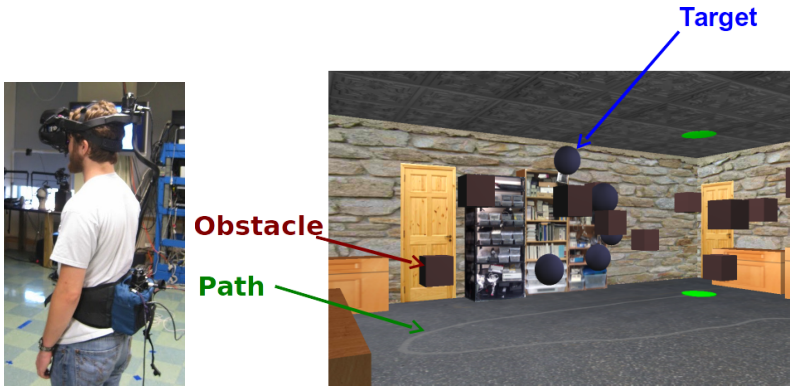

Figure 4.2: The second test domain. (Left) A human subject wears a head mounted display (HMD) and trackers for eyes, head, and body. (Right) The virtual environment as seen through the HMD. The red cubes are obstacles and the blue spheres are targets. There is also a gray path on the ground which the human subject were told to follow.

We gave subjects four types of task instructions, resulting in 4 experimental conditions:

- **Task 1**: Follow the path only and ignore objects
- **Task 2**: Follow the path and avoid the obstacles
- **Task 3**: Follow the path and collect targets
- **Task 4**: Follow the path, collect targets, and avoid obstacles.

Subjects received auditory feedback when running into obstacles or targets, but only when the objects were task relevant. Here we examined data collected from 4 human subjects. Each subject walked through the environment 8 times

for each experimental condition, resulting in 32 experimental trials. In each trial the configuration of objects was different.

We use Equation 3.5 as our objective function to recover w and γ. Our agent uses the distance and angle to the module instances as state information. We constrain the action set of the agent to be human-like; it takes discrete forward actions, ranging from turning left 90 degrees to turning right 90 degrees.

The results are shown in Figure 4.3. Weights are normalized for comparison between modules. It is clear that the estimated w agreed with our task instructions. We then trained an agent with the recovered w and γ, and let the agent navigate in the same environment. The resulting agent trajectories (shown in green) are compared with human trajectories (shown in black) in Figure 4.3.

Task	Agent	Angular Diff.	Log Likelihood
Path only	Modular	25.820	-3914.196
	Reflex	35.600	-3916.157
	Random	55.219	-3926.847
Obstacle + Path	Modular	33.988	-4950.079
	Reflex	63.884	-4985.290
	Random	55.717	-4989.314
Target + Path	Modular	33.918	-4855.531
	Reflex	37.176	-4838.832
	Random	55.012	-4909.531
All	Modular	39.034	-6175.692
	Reflex	45.307	-6164.702
	Random	55.961	-6221.075

Table 4.1: Evaluation on the modular agent's performance compared with two baseline agents.

We compared the performance of our agent with two baseline agents, shown in Table 4.1. The *Random Agent* takes an action randomly without considering state information. The *Reflex Agent* greedily chases the nearest target or avoids the nearest obstacle, depending on which is closer. We considered two evaluation metrics. The first is the *angular difference* of the policies between the human subjects and the agent. For every state-policy pair in the human data, we compared the action the human took to the action our agent would select in the same state, taking the difference in angle between the chosen actions. The second metric is the *logarithm of the likelihood*, which is the probability that the human data is generated by the learned parameters. The results are shown in Table 4.1. The modular agent is more similar to the human subjects than the other two agents in terms of angular difference. However, in the last two tasks, it has similar performance with the reflex agent using the likelihood metric.

We then look at differences of w and γ within subjects and between subjects in Task 4. The results are shown in Figure 4.4. Within-subjects consistency indicates if the same subject has similar w and γ in different trials of Task 4, measured by the confidence interval (the errorbar). Between-subjects consistency indicates if different subjects have similar w and γ on average in Task 4, measured by the mean value (the height of bar). For w, an interesting observation is that subjects may have different weights for modules, even though they are given the same task instruction. Subject #3 is different than the other subjects, as he/she clearly weighted collecting targets less and

following path more. For γ, we do not find any significant within-subjects or between-subject consistency.

4.3 Introduction

Weighted sum of actions [12].

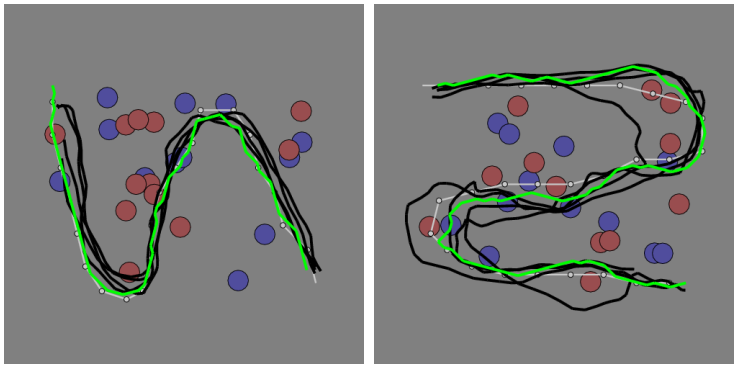

(a) Path only
Weights: [.035, .017, **.948**]
Discount factors: [.892, 0.181, .900]

(b) Path + Obstacle
Weights: [.000, **.227**, **.773**]
Discount factors: [.900, .134, .618]

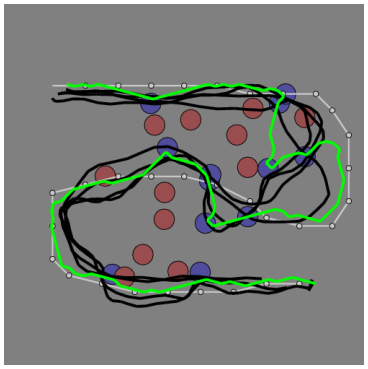

(c) Path + Target
Weights: [**.395**, .098, **.506**]
Discount factors: [.189, .100, .407]

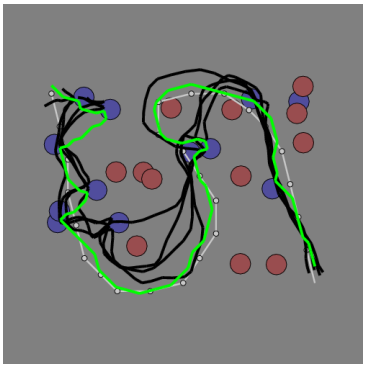

(d) Path + Target + Obstacle
Weights: [**.312**, **.180**, **.508**]
Discount factors: [.148, .100, .570]

Figure 4.3: The trajectories of the human subjects and the agent in four conditions. Targets are blue and obstacles are red. The black lines are trajectories of human subjects, and the green lines are trajectories of the RL agent trained using the recovered weights and discount factors. The weights and discount factors are shown in [Target, Obstacle, Path] format. The module weights that correspond to task instructions are bold.

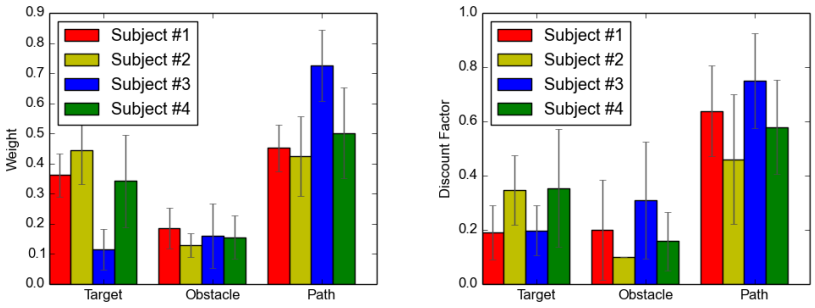

Figure 4.4: The weights (left) and discount factors (right) of different human subjects in Task 4. The error bars are 95% confidence intervals.

Chapter 5

Conclusion

Appendices

Bibliography

[1] Pieter Abbeel, Adam Coates, and Andrew Y Ng. Autonomous helicopter aerobatics through apprenticeship learning. *IJRR*, 2010.

[2] Pieter Abbeel and Andrew Y Ng. Apprenticeship learning via inverse reinforcement learning. In *Proceedings of the twenty-first ICML*, page 1. ACM, 2004.

[3] Dana H Ballard, Dmitry Kit, Constantin A Rothkopf, and Brian Sullivan. A hierarchical modular architecture for embodied cognition. *Multisensory research*, 26:177–204, 2013.

[4] Andrew G Barto and Sridhar Mahadevan. Recent advances in hierarchical reinforcement learning. *Discrete Event Dynamic Systems*, 13(4):341–379, 2003.

[5] Sooraj Bhat, Charles L Isbell, and Michael Mateas. On the difficulty of modular reinforcement learning for real-world partial programming. In *Proceedings of the National Conference on Artificial Intelligence*, volume 21, page 318. Menlo Park, CA; Cambridge, MA; London; AAAI Press; MIT Press; 1999, 2006.

[6] Justin Boyan and Andrew W Moore. Generalization in reinforcement

learning: Safely approximating the value function. *In NIPS*, pages 369–376, 1995.

[7] Jaedeug Choi and Kee-Eung Kim. Map inference for bayesian inverse reinforcement learning. In *NIPS*, pages 1989–1997, 2011.

[8] Jaedeug Choi and Kee-Eung Kim. Nonparametric bayesian inverse reinforcement learning for multiple reward functions. In *NIPS*, pages 305–313, 2012.

[9] Thomas G Dietterich. Hierarchical reinforcement learning with the maxq value function decomposition. *J. Artif. Intell. Res.(JAIR)*, 13:227–303, 2000.

[10] Christos Dimitrakakis and Constantin A Rothkopf. Bayesian multitask inverse reinforcement learning. In *Recent Advances in Reinforcement Learning*, pages 273–284. Springer, 2012.

[11] Kenji Doya, Kazuyuki Samejima, Ken-ichi Katagiri, and Mitsuo Kawato. Multiple model-based reinforcement learning. *Neural computation*, 14(6):1347–1369, 2002.

[12] Katie Genter, Shun Zhang, and Peter Stone. Determining placements of influencing agents in a flock. 2015.

[13] Samuel J Gershman, Bijan Pesaran, and Nathaniel D Daw. Human reinforcement learning subdivides structured action spaces by learning

effector-specific values. *The Journal of Neuroscience*, 29(43):13524–13531, 2009.

[14] Carlos Guestrin, Daphne Koller, and Ronald Parr. Multiagent planning with factored mdps. In *NIPS*, volume 1, pages 1523–1530, 2001.

[15] Carlos Guestrin, Daphne Koller, Ronald Parr, and Shobha Venkataraman. Efficient solution algorithms for factored mdps. *Journal of Artificial Intelligence Research*, pages 399–468, 2003.

[16] Masahiko Haruno, Tomoe Kuroda, Kenji Doya, Keisuke Toyama, Minoru Kimura, Kazuyuki Samejima, Hiroshi Imamizu, and Mitsuo Kawato. A neural correlate of reward-based behavioral learning in caudate nucleus: a functional magnetic resonance imaging study of a stochastic decision task. *The Journal of Neuroscience*, 24(7):1660–1665, 2004.

[17] Clay B Holroyd and Michael GH Coles. The neural basis of human error processing: reinforcement learning, dopamine, and the error-related negativity. *Psychological review*, 109(4):679, 2002.

[18] Mark Humphrys. Action selection methods using reinforcement learning. *From Animals to Animats*, 4:135–144, 1996.

[19] Leslie Pack Kaelbling, Michael L Littman, and Andrew W Moore. Reinforcement learning: A survey. *arXiv preprint cs/9605103*, 1996.

[20] Mitsuo Kawato and Kazuyuki Samejima. Efficient reinforcement learning: computational theories, neuroscience and robotics. *Current opinion in neurobiology*, 17(2):205–212, 2007.

[21] Sergey Levine, Zoran Popovic, and Vladlen Koltun. Nonlinear inverse reinforcement learning with gaussian processes. In *NIPS*, pages 19–27, 2011.

[22] Katharina Muelling, Abdeslam Boularias, Betty Mohler, Bernhard Schölkopf, and Jan Peters. Learning strategies in table tennis using inverse reinforcement learning. *Biological cybernetics*, 108(5):603–619, 2014.

[23] Gergely Neu and Csaba Szepesvári. Apprenticeship learning using inverse reinforcement learning and gradient methods. *UAI*, 2012.

[24] Andrew Y Ng, Stuart J Russell, et al. Algorithms for inverse reinforcement learning. In *ICML*, pages 663–670, 2000.

[25] Norihiko Ono and Kenji Fukumoto. Multi-agent reinforcement learning: A modular approach. In *Proceedings of the Second International Conference on Multi-Agent Systems*, pages 252–258, 1996.

[26] Deepak Ramachandran and Eyal Amir. Bayesian inverse reinforcement learning. In *Proceedings of the 20th IJCAI*, pages 2586–2591. Morgan Kaufmann Publishers Inc., 2007.

[27] Mark Ring and Tom Schaul. Q-error as a selection mechanism in modular reinforcement-learning systems. In *IJCAI*, volume 22, page 1452, 2011.

[28] Khashayar Rohanimanesh and Sridhar Mahadevan. Coarticulation: an approach for generating concurrent plans in markov decision processes. In *Proceedings of the 22nd ICML*, pages 720–727. ACM, 2005.

[29] Constantin A Rothkopf. Inferring human intrinsic rewards through inverse reinforcement learning. *Frontiers in Computational Neuroscience*, (50), 2013.

[30] Constantin A Rothkopf and Dana H Ballard. Modular inverse reinforcement learning for visuomotor behavior. *Biological cybernetics*, 107(4):477–490, 2013.

[31] Stuart Russell and Andrew Zimdars. Q-decomposition for reinforcement learning agents. In *ICML*, pages 656–663, 2003.

[32] Kazuyuki Samejima, Kenji Doya, and Mitsuo Kawato. Inter-module credit assignment in modular reinforcement learning. *Neural Networks*, 16(7):985–994, 2003.

[33] Nathan Sprague and Dana Ballard. Multiple-goal reinforcement learning with modular sarsa (0). In *IJCAI*, pages 1445–1447. Citeseer, 2003.

[34] Nathan Sprague, Dana Ballard, and Al Robinson. Modeling embodied visual behaviors. *ACM Transactions on Applied Perception (TAP)*, 4(2):11, 2007.

[35] Rainer Storn and Kenneth Price. *Differential evolution-a simple and efficient adaptive scheme for global optimization over continuous spaces*, volume 3. ICSI Berkeley, 1995.

[36] Rainer Storn and Kenneth Price. Differential evolution–a simple and efficient heuristic for global optimization over continuous spaces. *Journal of global optimization*, 11(4):341–359, 1997.

[37] Richard S Sutton and Andrew G Barto. *Introduction to reinforcement learning*. MIT Press, 1998.

[38] Richard S Sutton, Doina Precup, and Satinder Singh. Between mdps and semi-mdps: A framework for temporal abstraction in reinforcement learning. *Artificial intelligence*, 112(1):181–211, 1999.

[39] Philip S Thomas and Andrew G Barto. Motor primitive discovery. In *ICDL-EPIROB*, pages 1–8, 2012.

[40] M. H. Tong and M. M. Hayhoe. Modeling uncertainty and intrinsic reward in a virtual walking task. *Journal of Vision*, 14(10):5, August 2014.

[41] Eiji Uchibe, Minoru Asada, and Koh Hosoda. Behavior coordination for a mobile robot using modular reinforcement learning. In *IROS*, volume 3, pages 1329–1336. IEEE, 1996.

[42] Adam Vogel, Deepak Ramachandran, Rakesh Gupta, and Antoine Raux. Improving hybrid vehicle fuel efficiency using inverse reinforcement learning. In *AAAI*, 2012.

[43] Christopher JCH Watkins and Peter Dayan. Q-learning. *Machine learning*, 8(3-4):279–292, 1992.

[44] Brian D Ziebart, Andrew L Maas, J Andrew Bagnell, and Anind K Dey. Maximum entropy inverse reinforcement learning. In *AAAI*, pages 1433–1438, 2008.

[45] Brian D Ziebart, Nathan Ratliff, Garratt Gallagher, Christoph Mertz, Kevin Peterson, James A Bagnell, Martial Hebert, Anind K Dey, and Siddhartha Srinivasa. Planning-based prediction for pedestrians. In *IROS*, pages 3931–3936. IEEE, 2009.

Vita

Permanent address: 9905 Chukar Circle
Austin, Texas 78758

This thesis was typeset with LaTeX[†] by the author.

[†]LaTeX is a document preparation system developed by Leslie Lamport as a special version of Donald Knuth's TeX Program.